The Low pKa Value of Iron-Binding Ligand Tyr188 and Its Implication in Iron Release and Anion Binding of Human Transferrin

Xuesong Sun[1,2], Hongzhe Sun[1,2] , Ruiguang Ge[1,2], Megan Richter[3], Robert C. Woodworth[3], Anne B. Mason[3] and Qing-Yu He[1,2 *]

[1]Department of Chemistry, [2]Open Laboratory of Chemical Biology of the Institute of Molecular Technology for Drug Discovery and Synthesis, University of Hong Kong, Hong Kong; [3]Department of Biochemistry, University of Vermont, Burlington, VT 05405, USA

Abstract: 2D NMR-pH titrations were used to determine pKa values for four conserved tyrosine residues, Tyr45, Tyr85, Tyr96 and Tyr188 in human transferrin. The low pKa of Tyr188 is due to the fact that the iron-binding ligand interacts with Lys206 in open-form and with Lys296 in the closed-form of the protein. Our current results also confirm the anion binding of sulfate and arsenate to transferrin and further suggest that Tyr188 is the actual binding site for the anions in solution. These data indicate that Tyr188 is a critical residue not only for iron binding but also for chelator binding and iron release in transferrin.

Key words: HSQC NMR, pKa, anion binding, transferrin, tyrosine.

***Corresponding author**: Dr. Qing-Yu He, Tel: (852)2299-0787, Fax: (852)2817-1006, E-mail: **qyhe@hku.hk**

Abbreviations: hTF, human serum transferrin; hTF/2N, recombinant N-lobe of human transferrin comprising residues 1-337; BHK, baby-hamster kidney cells; HSQC, heteronuclear single-quantum coherence; Y45E etc, protein where the Tyr45 residue has been replaced with a Glu residue etc.

1. Introduction

Human serum transferrin (hTF) is a member of the transferrin family that functions as an iron-binding and iron-transport protein [1-3]. Iron in the ferric form is bound to hTF in plasma at neutral pH and transported into cells where it is then released to an unknown chelator in the acidic environment of the endosome. A large conformational change between the apo- and iron-bound forms of the N-lobe of hTF (hTF/2N), has been demonstrated by X-ray crystallographic analysis [4, 5]. When iron is released, the two domains of this lobe rotate 63° around a central hinge leading to an 'open' conformation. The N-lobe of hTF binds iron by coordinating it to the side chains of four amino acids, Asp63, Tyr95, Tyr188 and His249. The iron is further coordinated by two oxygens from the synergistic anion, carbonate. The flexibility of hTF is demonstrated by its ability to accommodate different metal ions and anions in the specific iron- and anion-binding sites [3, 6].

Extensive work has been carried out by a number of laboratories to understand the structure of the hTF/2N iron-binding site and the distinct functional roles that the four ligands Asp63, Tyr95, Tyr188 and His249 play in iron binding and transport (see review [6]). Of equal importance, the significance of synergistic and non-synergistic anion binding in the mechanism of iron binding and release has also received extensive investigation (see review [6] and recent publications [7-9]). We have previously shown that the two tyrosine ligands, especially Tyr188, play an important role in iron release and anion binding [10, 11].

In the present report we explore the chemical properties of the tyrosine residues in and near the iron-binding site to further characterize their roles in both iron and anion binding. Five mutants, Y45E, Y85F, Y95F, Y96F and Y188F were selected for the study; the two liganding residues, Tyr95 and Tyr188, and the "second shell" residue, Tyr85, have known

functions, whereas the Tyr45 and Tyr96 residues do not play a direct role in iron binding and therefore serve as controls. Each of these tyrosines is well conserved in the sequences of mammalian transferrins (Fig. 1) [1, 4]. Two-dimensional NMR of [^{13}C]-labeled samples has allowed a definitive assignment to be made for four of the five tyrosines. In addition, we generated titration curves as a function of pH and have measured anion-binding of both sulfate and arsenate by titration of the apo-protein with each. The low pKa value of the ligand Tyr188 and its implication in anion binding are discussed.

2. Experimental

2.1. Materials

All chemical reagents are of commercial quality. L-tyrosine-phenol-3,5,-$^{13}C_2$ (CLM-623) was obtained from Cambridge Isotope Laboratories (Andover, MA) and other biochemical materials were from Gibco-BRL, Sigma and Amerham Biosciences. Stock solutions of Hepes, KCl, Na_2SO_4, Na_2HAsO_4 and other buffers were prepared by dissolving the anhydrous salts in Milli-Q (Millipore) purified water and adjusting the pH with 1 M NaOH or HCl.

2.2. Expression and purification of proteins

The production and purification of hTF/2N and for each of the five tyrosine mutants, Y45E, Y85F, Y95F, Y96F and Y188F, has been reported previously in detail [7, 10, 12]. In order to obtain the ^{13}C-labelled protein for NMR experiment, L-[^{13}C]-tyrosine replaced the normal concentration of tyrosine in the custom DMEM/F12 medium. For the NMR experiments, samples of hTF/2N and each of the mutants were at a final concentration of 0.3-1.0 mM in a solution containing 0.5 M KCl, pH 7.4, with 50% D_2O, (unless specified in the text). The pH values were determined using a Corning 440 pH-meter, equipped with an Aldrich micro-combination electrode, and calibrated with standard buffers.

2.3. NMR spectroscopy and pH titration

[^1H, ^{13}C] heteronuclear single-quantum coherence (HSQC) two-dimensional spectra were acquired on a Bruker AV600 spectrometer at 600.13 MHz for ^1H channel and 150.9 for ^{13}C channel. Experiments were carried out at 310K with 96-256 increment, acquired using

1024 complex points in the proton dimension and 64-160 increments in the carbon dimension. The spectral widths were 2kHz and 7kHz for ^{1}H and ^{13}C, respectively. Sodium 3-(trimethylsilyl) propionate was used as a chemical-shift reference. All 2D spectra were processed using XWIN-NMR software, and prior to Fourier transformation the data were zero-filled to 2K x 2K data points. The 2D [^{1}H, ^{13}C] HSQC spectra for wild-type recombinant hTF/2N were obtained in the pH range of 6-10. Spectra for each sample were recorded at pH intervals of 0.2. Titration curves were fitted using the Origin 7.0 software (OriginLab Corporation).

2.4. Anion-Binding Titration

A Cary 3E UV-vis spectrophotometer with temperature control was used to monitor titration of the protein samples with the anions, sulfate and arsenate, as described previously [13]. Hepes buffer (50 mM, pH 7.4) served as the reference for scans from 320 to 230 nm. The absorbance vs anion concentration data were fitted by Origin 7.0 software using the equation for the Hill plot. An anion-binding constant for each the binding of sulfate and arsenate was obtained from this plot [13].

3. Results

3.1. NMR assignments of tyrosine residues

The 2D [^{1}H, ^{13}C] HSQC spectra of apo-hTF/2N and the five mutants, Y45E, Y85F, Y95F, Y96F, Y188F, are displayed in Figure 2. Cross-peaks for ten of the fourteen tyrosine residues are observed in these spectra, although there is considerable overlap for some of the peaks. The assignment of the cross-peaks for Tyr45, Tyr85, Tyr96 and Tyr188 was aided by the observation of the 2D NMR spectra of the four tyrosine mutants Y45E, Y85F, Y96F, and Y188F (Fig. 2). For Y45E, the peak at 7.62/118.29 ppm (^{1}H/^{13}C) was missing, and for Y85F, peak at 7.12/119.70 ppm was missing, thus establishing assignments for Tyr45 and Tyr85. Peaks for Tyr96 and Tyr188 can be assigned similarly. The chemical shifts for Tyr45, Tyr85, Tyr96 and Tyr188 are specified in Table 1. However, no change was observed in the 2D spectrum of the Y95F mutant compared with wild-type hTF/2N under the identical conditions, indicating the cross-peak overlap of Tyr95 with other tyrosine residues in hTF/2N. Attempts to identify the cross-peak of Tyr95 by comparing the 2D spectra generated using their Fe(III)- and In(III)-bound forms of WT-hTF/2N and the Y95F mutant also failed (data not shown). Therefore, we were able to further investigate the properties of four tyrosine residues, Tyr45, Tyr85, Tyr96 and Tyr188.

3.2. pH Titration and pKa determination

Titration of apo-hTF/2N with HCl obviously leads to protonation of Tyr residues. The chemical shifts of the Tyr resonances (cross peaks) were monitored to measure the amount of protonation as a function of the pH. The 2D HSQC NMR spectra for apo-hTF/2N at pH 7.4 and 8.3 are given in Figure 3 (A & B). The plots of ^{13}C chemical shifts against pH over the

whole range for each of the assigned tyrosines are given in Figure 4. The titration curves generated from ^{1}H chemical shifts have similar patterns, with the Tyr45 curve exhibiting a sharper shape. The curves were fitted using a Hill plot equation and the pKa values for each residue were extracted, as presented in Tables 2 & 3 respectively based on the ^{1}H and ^{13}C chemical shifts. The pKa values and Hill coefficients (n) derived from either the ^{1}H or ^{13}C chemical shifts are compatible. Surprisingly, three of the four pKa values are around 7, remarkably lower than the normal pKa of tyrosine (~10). In particular, both curve fittings with the ^{1}H and ^{13}C chemical shifts produced a pKa lower than 7 (average 6.91) for residue Tyr188. In addition, the Hill coefficients, n, for most of tyrosine residues are normally around 1 but the n = 2.41 for Tyr45, corresponding to the sharp shape of its titration curve.

3.3. Anion binding titration

The binding of anions to apo-hTF/2N has been well documented ([11] and ref. therein). In the present work, 2D HSQC NMR was used to monitor which tyrosine residue(s) are involved in anion binding in solution. When apo-hTF/2N was titrated with sulfate, the position of the Tyr188 cross-peak moved toward the high-field while the position of all the other cross peaks remained unchanged (Fig. 3C), strongly indicating the involvement of residue Tyr188 in the binding of sulfate. The chemical shift in the carbon dimension for Tyr188 plotted against the sulfate concentration is shown in Figure 5A.

In like manner apo-hTF/2N was titrated with the arsenate anion (AsO_4^{3-}). The 2D HSDC NMR spectrum in the presence of an equivalent of arsenate is shown in Figure 3D. The binding of arsenate elicited a similar pattern to that found for sulfate; namely that the Tyr188 peak moved up-field and the Tyr188 resonance became weak while the cross-peaks of

other tyrosine residues remained unchanged. The chemical shift of ^{13}C for the Tyr188 resonance plotted against the arsenate concentration is shown in Figure 5B. Fitting the titration curves for the binding of these two anions with the equation for the Hill plot yielded binding constants (K) of 890 M^{-1} for sulfate and 3020 M^{-1} for arsenate, an approximately three fold difference.

Arsenate binding to apo-hTF/2N was also confirmed by difference UV spectroscopic titration. The UV difference spectrum of apo-hTF/2N after adding arsenate exhibited the typical electronic spectral absorption: two negative absorbance bands at 245 and 298 nm and a small positive band at around 276 nm (data not shown), resembling the difference spectra of sulfate binding [11, 13]. The maximum spectral absorptions at 245 or 298 nm were plotted against increasing concentrations of arsenate and then fitted to a Hill plot equation. An arsenate binding constant of 15980 M^{-1} was calculated, which again is about three times of that reported for the binding of sulfate (K = 5840 M^{-1}) [11]. It should be pointed out that the K values derived from the NMR titration are smaller than those derived from absorbance spectral titration. The reason is that the protein solution for NMR titration contained 0.5 M KCl in which anion chloride competes with sulfate or arsenate for anion binding to Tyr188, leading to small K values observed for sulfate and arsenate bindings.

4. Discussion

An essential feature of iron binding and transport by transferrin is its pH dependence. This iron release cycle of the hTF N-lobe is characterized by a conformational change between "open" and "closed" forms. Much work has suggested that this iron release process involves the protonation of several key amino acid residues around the metal-binding site within the binding cleft [5, 6, 14]. Investigations have been concentrated on the di-lysine pair (Lys206-Lys296) that bridges the binding cleft and the iron ligand His249 for their particular chemical properties. Once protonated, the Lys206-Lys296 pair is a driving force to open the cleft [11, 14]. Protonation of His249 is also clearly a factor in the mechanism of iron release in this lobe [5]. The present study focuses on the tyrosine residues residing in the iron binding site and along the cleft to further elucidate their role in the pH-sensitive iron release process.

Titration of apo-hTF/2N with acid changed the protonation states of the tyrosine residues, allowing us to monitor the change in chemical-shifts of the tyrosine peaks in the NMR spectra and providing a determination of the pKa values for each of the four assigned tyrosine residues. All four pKa values for Tyr45, Tyr85, Tyr96 and Tyr188 are considerably lower than those found for "normal" tyrosine residues in other proteins (pKa ~10) [15-18]. The low pKa values of tyrosines are obviously due to the electrostatic interactions with the neighboring groups. For example, Tyr85 has a higher pKa than the other three because that the OH of Tyr85 residue forms an H-bond with the negative Glu83 residue [5]. The low pKa for Tyr188 is most likely due to the H-bond interaction between Tyr188 and the positive residue Lys206 in the apo-hTF/2N molecule [5]. Also, the proton sharing between Tyr96 and Gln245 (2.81 Å distance) is probably the reason for the low pKa of Tyr96 [5].

As one would expect, the Hill coefficients for most of tyrosine residues evaluated are close to 1, indicating that a single proton is involved in the titration of each phenolic OH. However, a much higher Hill coefficient (n ~ 2.4) was derived for Tyr45, suggesting that other residues cooperatively participated in the ionization process of Tyr45 titration ([19] and ref. therein). Careful inspection of the structure around Tyr45 in the open form of hTF/2N (1BP5) reveals that residues Glu15, Asp63 and His249 are within the range of 6Å of the tyrosine side chain. It is therefore likely that these neighboring groups co-titrated with Tyr45 residue giving rise to the sharp curve. In this regard, the low pKa of Tyr45 may be an apparent value for the composite of more than one proton dissociation from these residues.

Our current finding of low pKa values in a range of 7 ~ 8 for the tyrosine residues is also perfectly consistent with the result derived from an ultraviolet absorption titration of apo-transferrin in which an apparent pKa of 7.57 for tyrosine residues was obtained [20]. The apparent pKa of 7.57 can be viewed as an average value for all the tyrosines participating in the titration-related ionization process. However, a recent theoretical calculation suggested that all involved tyrosine residues have pKa higher than 9.5 in both apo-open and apo-closed forms of hTF/2N [21]. These theoretical pKa's are actually close to those for free tyrosines and greatly different from the experimental data obtained. The substantial difference between the experimental findings and the modeling study may be due to the fact that the theoretical calculations are based on the crystal structure.

In terms of iron binding and release from hTF, we do not observe any significance for the low pKa values of residues Tyr45 or Tyr96. However, the low pKa of Tyr188 is an important property for the liganding residue. A pKa of 6.91 for Tyr188 suggests that even at a pH lower than 7, the iron ligand Tyr188 is susceptible to de-protonation. Structurally, besides

its H-bond interaction with Lys206 in apo-hTF/2N, Tyr188 has a short connection with Lys296 (3.17 Å) in the closed form of hTF/2N [4]. This implies that the de-protonated state of Tyr188 is stabilized in both the open and closed conformation of the protein. This structural arrangement and the low pKa of Tyr188 favors the protein with iron binding in the open form and tends to disfavor iron release from the protein in the iron-bound closed conformation.

The structural interaction with the di-lysine pair Lys206-Lys296 means that Tyr188 plays a key role in anion binding. Our earlier study suggested that Tyr188 forms a combination anion-binding site with Lys296 and Lys206 in a closed conformation in which Lys296 is believed to be the core for anion binding and Tyr188 is the main reporter for the electronic spectral change upon binding anion [11]. The current NMR data for the titration with sulfate confirms that Tyr188 is the only observable tyrosine residue directly involved in anion binding. All of these observations lead to the conclusion that the Tyr188-Lys206 pair is probably the initial anion-binding site in the open structure of hTF/2N. In the closed conformation, Lys296 is brought into proximity and plays a crucial role in anion binding. It seems that this site acts as a pathway to bring in a synergistic anion for iron binding and also in reverse to introduce a chelator near the iron-binding site for iron release.

In conclusion, we have used 2D NMR spectroscopy and single-point mutants of hTF/2N to definitely assign the four tyrosine residues, Tyr45, Tyr85, Tyr96 and Tyr188, and observed the behaviors of these tyrosines under different pHs and concentrations of anions. The low pKa values for all four tyrosines derived from the pH titration are accounted for by neighboring electrostatic environments. In particular, the close connection of Tyr188-Lys206 and Tyr188-Lys296 respectively in the open and closed structures of hTF/2N stabilizes Tyr188 in any de-protonated state in either conformation; the low pKa of Tyr188 would

therefore favors iron binding but disfavors iron release from the protein. Our data also validates the anion binding to apo-transferrin and further demonstrates the exact location of the anion binding. These data implicate the importance of Tyr188 in both iron binding and release in human transferrin.

Acknowledgements

This work was supported by Hong Kong Research Grants Council Grants HKU 7227/02M (to Q.Y.H.) and, and University Grant 10205307 (to Q.Y.H.), the Department of Chemistry, and the Areas of Excellence scheme of Hong Kong University Grants Committee and by USPHS Grant R01 DK21739 (to A.B.M.). We thank Dr. Hongyan Li for technical assistance.

References

[1] Evans,R.W., Crawley,J.B., Joannou,C.L., & Sharma,N.D. (1999) Iron Proteins. In *Iron and Infection:Molecular, Physiological and Clinical Aspects* (Bullen,J.J. & Griffiths,E., eds), pp. 27-86. John Wiley and Sons, Chichester.

[2] Aisen,P. (1998) Transferrin, the Transferrin Receptor, and the Uptake of Iron by Cells. In *Iron Transport and Storage in Microorganisms, Plants and Animals* (Sigel,A. & Sigel,H., eds), pp. 585-631. Marcel Dekker, Inc, New York.

[3] Baker, E. N., (1994) Adv. Inorg. Chem. 41**,** 389-463.

[4] MacGillivray, R. T. A., Moore, S. A., Chen, J., Anderson, B. F. et al, (1998) Biochemistry 37**,** 7919-7928.

[5] Jeffrey, P. D., Bewley, M. C., MacGillivray, R. T. A., Mason, A. B. et al, (1998) Biochemistry 37**,** 13978-13986.

[6] He,Q.-Y. & Mason,A.B. (2001) Molecular aspects of release of iron from transferrin. In *Molecular and Cellular Iron Transport* (Templeton,D.M., ed), pp. 95-123. Marcel Dekker, Inc., New York.

[7] Adams, T. E., Mason, A. B., He, Q. Y., Halbrooks, P. J. et al, (2003) J. Biol. Chem. 278**,** 6027-6033.

[8] Zak, O., Ikuta, K., Aisen, P., (2002) Biochemistry 41**,** 7416-7423.

[9] Ikuta, K., Zak, O., Aisen, P., (2004) Int. J. Biochem. Cell Biol. 36**,** 340-352.

[10] He, Q.-Y., Mason, A. B., Woodworth, R. C., Tam, B. M. et al, (1997) Biochemistry 36**,** 14853-14860.

[11] He, Q.-Y., Mason, A. B., Tam, B. M., MacGillivray, R. T. A. et al, (1999) Biochemistry 38**,** 9704-9711.

[12] He, Q.-Y., Mason, A. B., Woodworth, R. C., Tam, B. M. et al, (1998) J. Biol. Chem. 273**,** 17018-17024.

[13] Cheng, Y. G., Mason, A. B., Woodworth, R. C., (1995) Biochemistry 34**,** 14879-14884.

[14] Dewan, J. C., Mikami, B., Hirose, M., Sacchettini, J. C., (1993) Biochemistry 32**,** 11963-11968.

[15] Davis, J. P., Zhou, M. M., Van Etten, R. L., (1994) Biochemistry 33**,** 1278-1286.

[16] Li, Y. K., Kuliopulos, A., Mildvan, A. S., Talalay, P., (1993) Biochemistry 32**,** 1816-1824.

[17] Fujii, S., Akasaka, K., Hatano, H., (1981) Biochemistry 20**,** 518-523.

[18] Canioni, P. & Cozzone, P. J., (1979) FEBS Lett. 97**,** 353-357.

[19] Woodworth, R. C., Butcher, N. D., Brown, S. A., Brown-Mason, A., (1987) Biochemistry 26**,** 3115-3120.

[20] Clarkson, J. & Smith, D. A., (2001) FEBS Lett. 503**,** 30-34.

[21] Rinaldo, D. & Field, M. J., (2003) Biophys. J. 85**,** 3485-3501.

Table 1. Summary of ^{1}H– and ^{13}C- NMR chemical shifts for the ^{13}C tyrosine-labeled residues in hTF/2N. Conditions: *T* = 310K and pH = 7.4.

Peak	^{1}H (ppm) ± SD	^{13}C (ppm) ± SD
Tyr45	7.622 ± 0.003	118.291 ± 0.017
Tyr85	7.129 ± 0.002	119.702 ± 0.007
Tyr96	7.048 ± 0.010	117.413 ± 0.002
Tyr188	7.280 ± 0.004	118.454 ± 0.005

Table 2. **pKa values for four tyrosine residues in apo-hTF/2N based on ^{1}H chemical shift**. **Conditions: *T* = 310K.**

Residue	p*K*a ± SD	n[a] ± SD	δ_+[b]	δ_0[b]	$\Delta\delta$[c]
Y45	6.86 ± 0.01	2.41 ± 0.24	7.679	7.620	0.059
Y85	8.14 ± 0.02	0.84 ± 0.13	7.192	6.970	0.222
Y96	6.98 ± 0.02	1.12 ± 0.07	7.088	7.026	0.062
Y188	6.96 ± 0.04	0.86 ± 0.09	7.364	7.209	0.155

[a]n , Hill coefficient.

[b]δ_+ and δ_0 are the limiting chemical shifts in ppm for the protonated and deprotonated species, respectively.

[c]$\Delta\delta$ is the chemical shift change ($\Delta\delta_+ - \delta_0$)

Table 3. **pKa values for four tyrosine residues in apo-hTF/2N based on the ^{13}C chemical shift**. **Conditions: *T* = 310K**

Residue	p*K*a ± SD	n[a] ± SD	δ_+[b]	δ_0[b]	$\Delta\delta$[c]
Y45	7.09 ± 0.04	2.40 ± 0.15	118.677	118.230	0.447
Y85	8.01 ± 0.07	0.93 ± 0.04	120.139	118.401	1.738
Y96	7.06 ± 0.08	1.16 ± 0.12	118.043	117.258	0.785
Y188	6.86 ± 0.05	0.96 ± 0.08	119.056	118.346	0.710

[a]n , Hill coefficient.

[b]δ_+ and δ_0 are the limiting chemical shifts in ppm for the protonated and deprotonated species, respectively.

[c]$\Delta\delta$ is the chemical shift change ($\Delta\delta_+ - \delta_0$)

Figure legend

Figure 1. Structure of the apo-form of human transferrin N-lobe (1BP5).
The locations of five tyrosine residues, Y45, Y85, Y95, Y96 and Y188 are shown.

Figure 2. 2D (^{1}H, ^{13}C) HSQC NMR spectra of [^{13}C] tyrosine –labeled apo-hTF/2N and five mutants. Conditions: T = 310K and pH = 7.4.
Arrows point out the corresponding missed peaks in each matant proteins.

Figure 3. Representative 2D HSQC NMR spectra of apo-hTF/2N showing the chemical shift movement at different pH and anion concentrations. Conditions: T = 310K.

Figure 4. ^{13}C NMR titration curves for Tyr45, Tyr85, Tyr96 and Tyr188 of wild-type apo-hTF/2N. Conditions: T = 310K.

Figure 5. ^{13}C NMR titration curves of Tyr188 of wild-type apo-hTF/2N when titrated with sulfate and arsenate .Conditions: T = 310K and pH = 7.4.

Figure 1. Structure of the apo-form of human transferrin N-lobe (1BP5).

The locations of five tyrosine residues, Y45, Y85, Y95, Y96 and Y188 are shown.

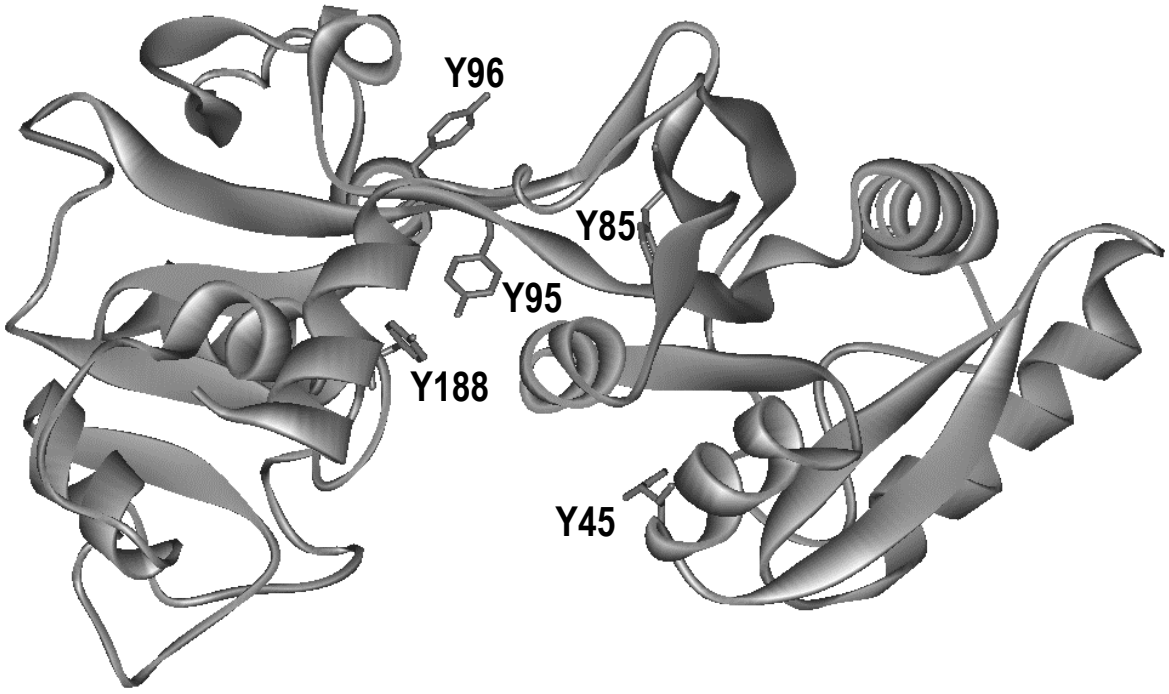

Figure 2. 2D (^{1}H, ^{13}C) HSQC NMR spectra of [^{13}C] tyrosine –labeled apo-hTF/2N and five mutants. Conditions: *T* = 310K and pH = 7.4.

Arrows point out the corresponding missed peaks in each matant proteins.

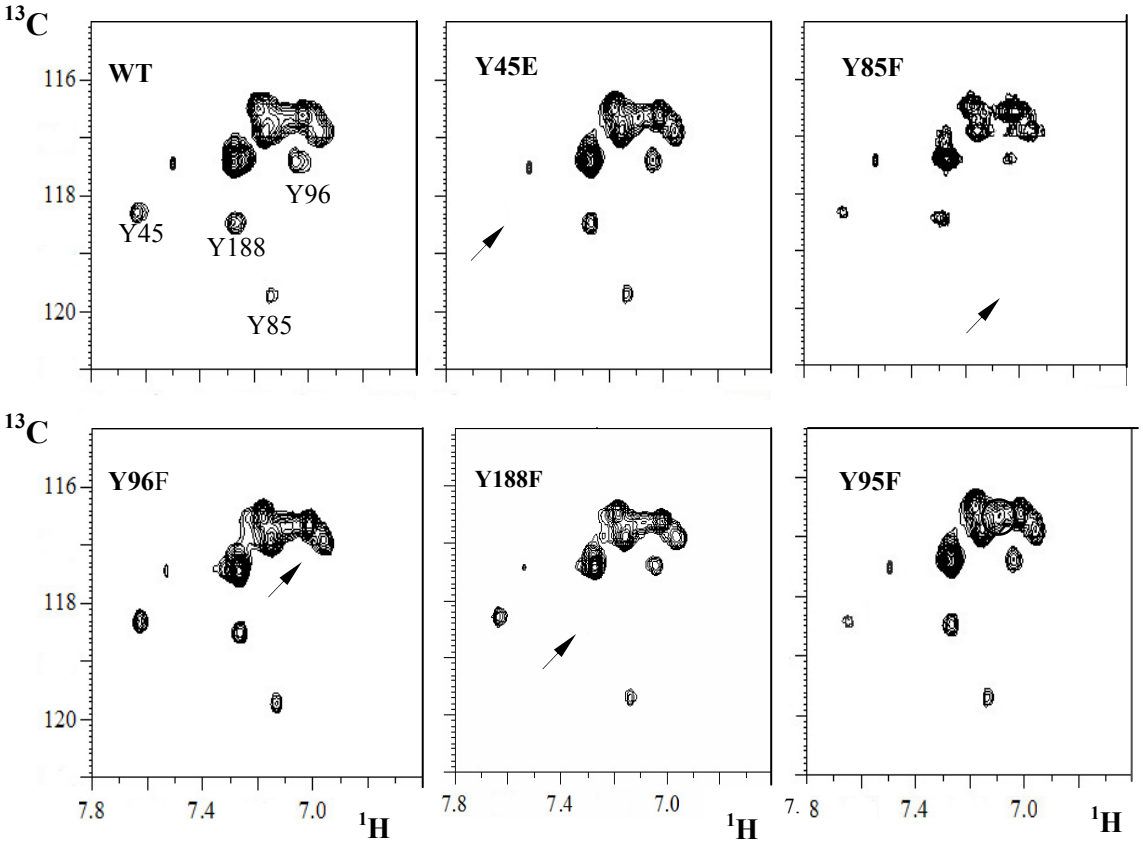

Figure 3. Representative 2D HSQC NMR spectra of apo-hTF/2N showing the chemical-shift movement at different pH and anion concentrations. Conditions: T = 310K.

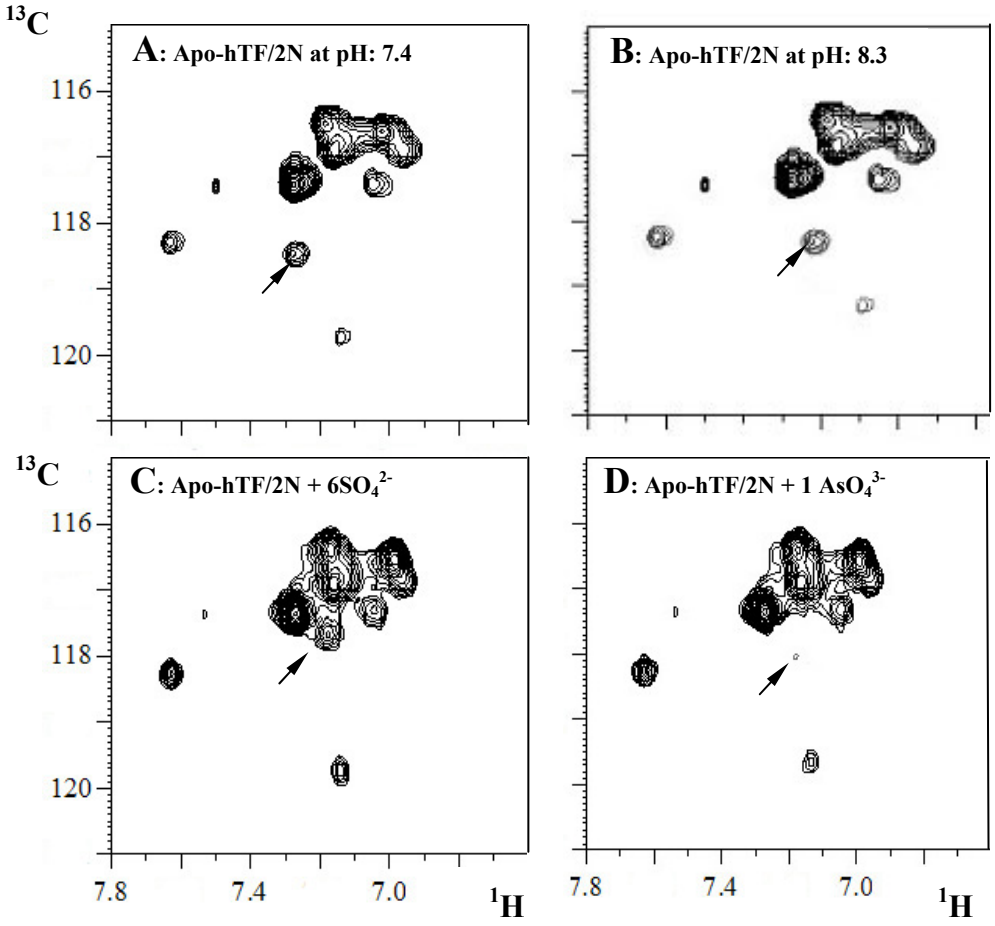

Figure 4. ^{13}C NMR titration curves for Tyr45, Tyr85, Tyr96, and Tyr188 of wild-type apo-hTF/2N. Conditions: T = 310K.

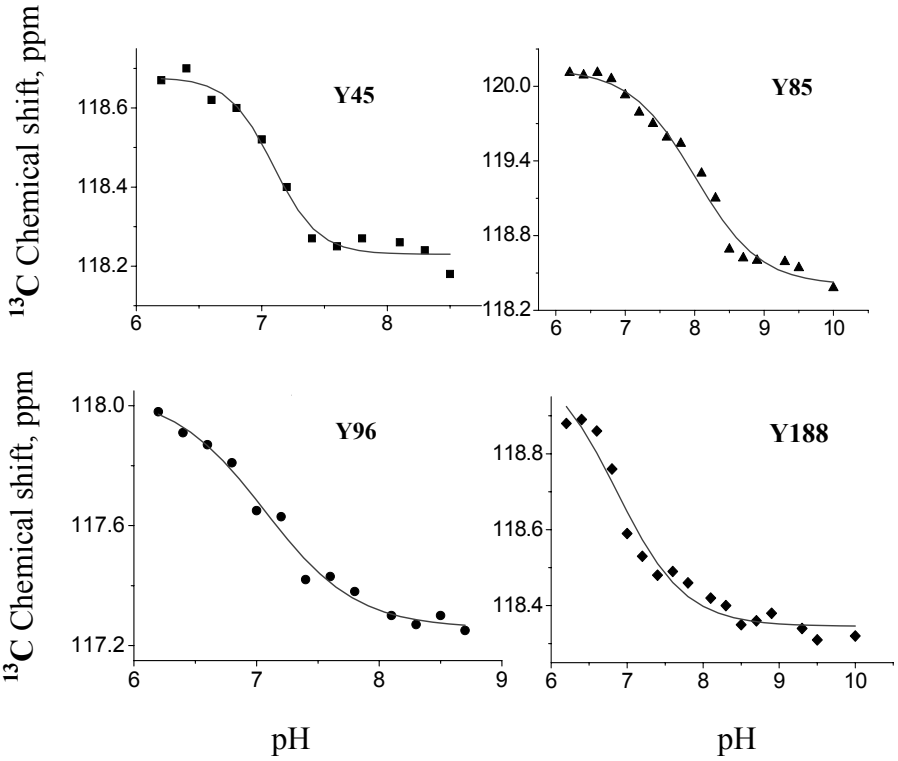

Figure 5. **^{13}C NMR titration curves of Tyr188 in wild-type apo-hTF/2N when titrated with sulfate and arsenate .Conditions: T = 310K and pH = 7.4.**